Analytical Methods in Plasma Diagnostic by Optical Emission Spectroscopy: A Tutorial Review

H. H. Ley*, A. Yahaya, R. K. Raja Ibrahim

Department of Physics, Universiti Teknologi Malaysia, 81310 Skudai Johor.

*Corresponding email: leyhh@hotmail.com

Abstract

This article reviews on the basic data processing technique and plasma diagnosis method by optical emission spectroscopy. The review is focused on the physical concepts of an analysis methods and its application to determine the plasma parameters. Processing procedures such as signal averaging and spectrum smoothing technique such as boxcar are discussed. Next, conditions such as local thermodynamic equilibrium plasma were briefly discussed with the method available to assess its existence. Similarly, the available techniques to quantitatively determine optically thin condition of spectral line are considered including method to calculate the suitable time window for a spectral line to be optically thin. Measurement techniques of plasma temperature and electron density were compared and contrast to gauge the advantages of each technique.

Keywords: analytical methods; plasma diagnostic; optical emission spectroscopy

1. INTRODUCTION

The word 'plasma' which means jelly in Greek was coined by Nobel Laureate Irving Langmuir who pioneered the study of this new state of matter. Plasma is simply an ionised gas consisting positive and negatively charged particles of roughly equal charge density. As such, plasma can be formed when any gaseous state is heated to a sufficient temperature such that the particles collide against each other and knocking off electrons in the process producing a mixture of ions and electrons.

Plasma can be categorised into high temperature known as fusion plasma, and low temperature plasma. This review paper will focus only for the latter group of plasma. Low temperature plasmas can be further divided into plasma that is in thermal equilibrium and those which are not in thermal equilibrium. The term thermal equilibrium refers to when the temperature of all plasma species such as electrons, ions, neutral particles, is the same [1-7]. However, this condition is only true for stellar and fusion plasma and almost never achieved in laboratory plasma. For that matter, a more lenient condition called the 'local thermal equilibrium', or LTE in short, is used to imply that temperature for all plasma species are the same for a localised area in the plasma.

Optical emission spectroscopy (OES) is commonly employed in the diagnosis of laboratory plasma such as gas discharge plasma, inductively coupled plasma (ICP), or laser induced plasma (LIP). Numerous analytical techniques have been established to determine the plasma properties such as electron density, plasma temperature, element recognition and quantification of elements present in the plasma. For instance, the Laser Induced Breakdown Spectroscopy (LIBS) technique is widely used to study elemental composition of a sample. Gondal *et al.*[8] and Trevizan *et al.*[9] demonstrated such technique to determine the amount of poisonous metal presence in wastewater from paint manufacturing plant and the amount of micronutrient in plant material respectively. The details on LIBS experimental setup, conditions, and analysis are discussed in great length in [1, 2, 10].

Various studies of ICP plasma system such as argon [11, 12], or even combinations of several molecules system [13] were analysed via OES to obtain the plasma properties. Review on mathematical procedures for background correction and analysis in ICP is described by E. H. Van Veen [14]. Similarly, myriads of work have also been done on OES for glow discharge plasma which includes development of mathematical models to describe the plasma [15-17], and a review on its applications [7].

Thus, the purpose of this paper is to describe the basic analytical techniques applied in the research on plasma diagnosis by OES in terms of data processing and determination of plasma properties. Although a few books by Griem [3], Hutchinson [4], and Kunze [5] may have explained extensively the plasma diagnosis method and its underlying physical principles, it is necessary to provide discussion on data pre-treatment

method and details on analysis condition. This review would serve to provide and expose initial knowledge to new researchers who are about to embark into this field of study.

2. PRE-PROCESSING OF EXPERIMENTAL DATA

Generally, dark background spectrum component is measured without the light source on, and it can be easily eliminated using the software provided by the spectrometer or it can be done manually by measuring the dark spectrum separately and subtracting it from the spectrum obtained. Note that the exposure time for dark background must match that of data collection, for instance, data collected with exposure time of 1 second will need to be applied with dark background recorded with one second exposure time. Figure 1 shows the comparison of spectrum with dark background subtracted and without subtracting the dark background.
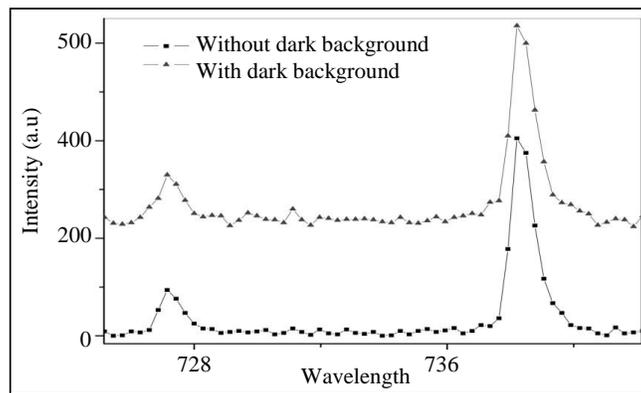

Figure 1: Mercury glow discharge spectra

2.1 Signal Averaging

The spectral information obtained from the spectrometer is encoded in the form of electrical signal. Hence, the presence of an undesirable component in the signal called noise is inevitable and it will also impede the accuracy and interpretation of the data. The factor which contributes to noise and methods to overcome it are explained briefly by [18]. For that, the quality of a spectral measurement is measured by signal-to-noise ratio, *S/N* defined as;

$$S/N = \text{average signal magnitude / rms noise}$$

A good spectrum is portrayed by a high signal-to-noise ratio, which can be done by a process called signal averaging. This process is conducted by repeated scanning and taking the summation of individual spectra. Assuming random distribution of noise, time coherent signals improve linearly with number of scans *N*, mathematically expressed as;

$$\text{Signal magnitude} = C_1 N \tag{1}$$

where C_1 is proportionality constant

On the other hand, the average magnitude of random noise increases proportional to the square roots of number of scans given by;

$$\text{Noise magnitude} = C_2 N^{1/2} \tag{2}$$

where C_2 is proportionality constant

Dividing (1) by (2) yields the signal-to-noise ratio;

$$\frac{signal}{noise} = \frac{C_1 N}{C_2 N^{1/2}} = CN^{1/2} \tag{3}$$

The results of equation (3) where C is a constant, shows that the signal-to-noise ratio is proportional to the square roots of the number of scans. The effect of averaging on spectrum is illustrated in Figure 2.
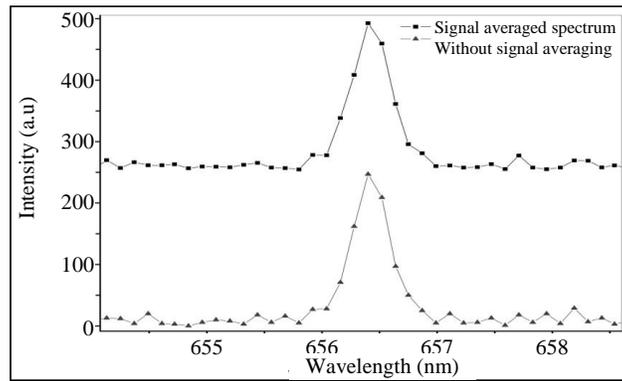

Figure 2: 10 scans are applied in this case hence the average spectrum (top) appeared to be less 'noisy'. The vertical axis of the spectrum is shifted to avoid spectra from coinciding.

2.2   Signal Smoothing

Despite performing signal averaging, a spectrum may still appear to be 'noisy' and this can be overcome by signal smoothing process. Note that there are a few methods to perform signal smoothing but in this case we will only elaborate on boxcar averaging which is a simpler method and usually provided in the accompanying software of a spectrometer compared to the others such as polynomial smoothing, Savitzky-Golay smoothing or moving average method. Boxcar averaging is carried out by replacing a centroid average value for a spectral data which are divided into groups of equally spaced and discrete bands [18]. The degree of smoothing is proportional to the number of points averaged. However, over smoothing of spectrum by this method will introduce distortion and loss of spectral resolution. Comparison of different degree of boxcar smoothing applied on the same spectrum is shown in Figure 3. Further explanation of other smoothing method such as moving average method and Savitzky-Golay smoothing are explained in detail in reference [18].
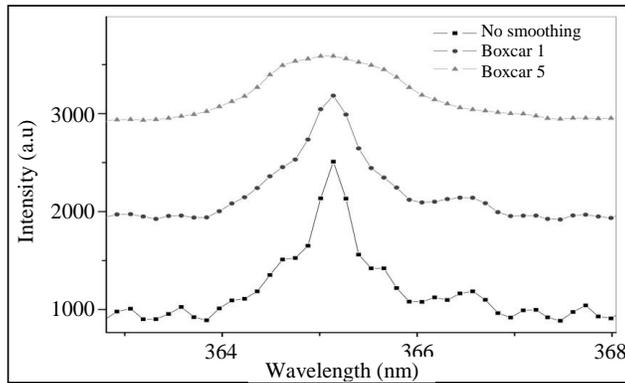
Figure 3: Comparison of different degree of boxcar smoothing performed via Ocean Optic's spectrometer software, Spectra Suite. Different degrees of boxcar spectrum are shifted on the y-axis to avoid data overlapping.

2.3   Signal Stacking

This method is employed to differentiate data points from noises. From equation (1), the time coherent signal magnitude is directly proportional to the number of scans which is conducted by repeated scans and summing each individual spectrum to a stacked spectrum. This spectrum will unveil any data points which initially have intensities comparable to the noise in one scan. In Figure 4, clearly data point increases linearly with the number of spectra employed in the summation which unveils a data peak close to 715nm which is only distinguishable after 10 sets of spectra applied. This method is used to improve the visibility of peaks that corresponds to data and not to be used for analysis purposes such as to determine the plasma parameters like temperature or electron density. For this matter, signal-averaged spectrum should be utilised to ensure accuracy of the results.
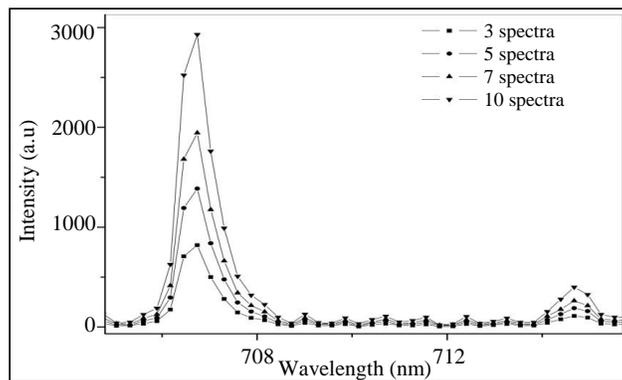

Figure 4: Comparison of different numbers of spectra used in signal summation

3.   LOCAL THERMAL EQUILIBRIUM

The radiative behaviour of the atomic species in any plasma can only be predicted if the expected population of its myriad possible states are known. The condition called thermal equilibrium is satisfied if and only if the atoms obeys Boltzmann distribution for every possible states, and the radiation energy density for all transition has the blackbody level of the system temperature [19, 20].

However, this condition is difficult to be achieved by laboratory plasma, and hence LTE is taken into consideration. LTE is a state where Boltzmann and Saha equations which governs distribution of energy level excitation and ionization temperature respectively are equal to Maxwell-Boltzmann distribution of free-electron velocities [1, 19-21].

Upon achieving LTE, one describes the plasma by a common temperature T and the collisions with electrons must dominate over the radiative processes thus requires the existence of sufficiently large electron density in order for this condition to hold. For that matter, a criterion as proposed by McWhirter which is based on the existence of critical amount of electron density required such that LTE condition to be valid, as demonstrated in most researches [1, 22-27], given by equation (4);

$$N_e \geq 1.6 \times 10^{12} T^{\frac{1}{2}} (\Delta E)^3 \, cm^3 \tag{4}$$

In equation (4), N_e, T, and ΔE refers to the electron density, plasma temperature, and energy gap (in electron volt) respectively. However, equation (4) is a necessary but not a decisive condition to solely prove the existence of LTE in the plasma due to the fast evolution and temperature decrease in the case of laser induced plasma [23].

Several methods other than McWhiter's criterion can be used to ensure the existence of LTE, which are generally based on experimental plasma temperature. First is via comparison of ionization and excitation temperatures obtainable from Saha-Boltzmann and Boltzmann equation. The other one is judged from the concurrence between Boltzmann distribution and experimental spectral intensities that is projected in the linearity of the Boltzmann plot [1, 4, 5, 23].

3.1   Optically Thin Condition

In order to characterize plasma by means of optical emission spectroscopy, optically thin condition of a spectral line is required. This is due to the fact that an optically thick line would imply self-absorption and saturation in the line profile, hence leading to a distorted or asymmetrical peak in the spectrum and causes incorrect calculations for electron density and temperature [1-5].

One of the most common methods to inspect the optically thin condition is via the linearity of Boltzmann plot [5]. Data point which shows large deviation from the linear

relationship implies the corresponding lines which are optically thick. Another method to verify for optically thin condition is by using the so called two lines ratio method (section 4.1) , where the experimental intensity ratio of two lines selected are compared with the intensity calculated theoretically [21]. Departure of the experimental ratio from theoretical one suggests an optically thick line.

3.2   Spectral Broadening

Theoretically, electron transition from higher to lower energy level will release the energy in the form of photon corresponds to the difference in the energy between the levels and one would then expect a sharp line on a wavelength value shown in a spectrum. However in reality, there will generally be a symmetrical distribution over a mean wavelength known as spectral broadening. This phenomenon is caused by several factors such as pressure broadening, Doppler broadening, natural broadening and Stark broadening.

Under no other external factor which affects broadening, spectral lines are in the form of Gaussian distribution with central wavelength value λ and full width at half maximum (FWHM), denoted as $\Delta\lambda_{1/2}$. This is caused by natural broadening which cannot be eliminated. From Heisenberg uncertainty principle;

$$\Delta E \Delta t \geq \frac{\hbar}{2} \tag{5}$$

Any excited species exist in excited state for a finite lifetime before it de-excites to lower energy level. From equation (5), it follows that a finite value of Δt implies an uncertain value for ΔE, which results in the energy level appear to be fuzzy.

The shift in spectral lines as a result from either varying or constant electric field strength is called Stark shift, and thus the name Stark broadening. [3-5, 19, 20] The shift is proportional to the strength of electric field strength for the case of first order which is also known as linear Stark effect, where as for second order or quadratic Stark effect it is proportional to square of field strength. In addition to Stark effect, another line broadening also by similar mechanism called internal Stark effect has larger influence on the spectral profile. This effect is due to fluctuating electric field in the plasma since the radiating atoms are surrounded by electrons and ions. The electric field of nearby particles constitutes a perturbing effect especially on the energy levels close to the continuum, or an applied external electric field, where shifting and splitting of atomic levels will occur and contributes to spectral broadening.

As implied from the name, Doppler effects take place when there are relative movements between the observer and emitter. In this case, the observer is the spectrometer, hence atoms moving towards the spectrometer while emitting light will causes a blueshift in the light detected by spectrometer, and redshift for atoms moving

away from the spectrometer. This effect is due to random motion of particles which can be reduced by lowering the temperature of the system.

Another contributor in spectral broadening is the collisions between neighbouring particles in the plasma which in turn mutually disturb one another's electric fields. This type of broadening is also known as pressure broadening that varies proportionally with the pressure and composition of the gas. It is to be noted that there are few other broadening mechanisms but are not discussed as the broadening effect contributed is insignificant. Hence, it can be inferred that the greatest line broadening is caused by Doppler and internal Stark effect. For the case where Doppler broadening dominates, the spectral line follows Gaussian distribution where as for Stark broadened line depicts Lorentzian distribution.

4.0   DETERMINATION OF TEMPERATURE

The temperature of ions and electrons is directly proportional to the average random kinetic energy. In thermal equilibrium, distribution of velocities for each type of particles is governed by Maxwell distribution. As mentioned earlier, thermal equilibrium condition is difficult to be achieved by laboratory plasma. In this case when LTE is considered, we associate the same temperature for atoms, ions, and electrons in the plasma. However in the absence of LTE, the electrons, ions and atoms in the plasma will not achieve equilibrium and each of them is characterised by its own temperature. Hence, the term plasma temperature refers to temperature of the plasma as a bulk, contributed mainly by the slow moving atoms and ions due to the larger mass compared to electrons.

The four most commonly used methods for the determination of temperature are the ratio method, Boltzmann plot, Saha-Boltzmann equation, and Doppler broadening. However, plasma temperature can also be determined via other methods such as continuum-line spectrum [1, 11], and numerical modelling [12, 28].

4.1   Ratio Method

The simplest approach in determining temperature is done by taking the intensity ratio of two spectral lines, provided that the population densities of the lines in upper level are in LTE. Take note that the temperature determined from this method refers to excitation temperature hence if LTE condition holds, the temperature is then known as electron temperature [1]. The intensity of the spectral line which is assumed to be optically thin is given by;

$$I_{ij} = \frac{hcA_{ij}g_j n}{\lambda_{ij}U(T)} e^{(\frac{E_j}{kT})}$$ (6)

Where $I_{i,j}$ and λ_{ij} is the intensity and wavelength corresponds to transition from i to j respectively, h is the Planck's constant, c is the speed of light, number density of emitting species n, partition function $U(T)$, A_{ij} is the transition probability between level i and j,

Boltzmann's constant k, excitation temperature T, g_j is the statistical weight of upper energy level and E_j upper energy level in eV unit.

Next, taking the intensity ratio of two spectral lines of the same species and ionization stage, the constants will be cancelled out yielding the relationship as demonstrated in [1, 21, 22, 25, 30, 33];

$$\frac{I_1}{I_2} = \frac{g_1}{g_2}\frac{A_1}{A_2}\frac{\lambda_2}{\lambda 1}e^{\left[-\left(\frac{E_1-E_2}{kT}\right)\right]}$$ (7)

where I is the intensity, g is the statistical weight, A is the transition probability, λ is the wavelength, E is the energy of excited state in eV and k is Boltzmann constant. The subscript 1 and 2 refer to the spectral lines of the same element selected. Figure 5 and Table 1 are the corresponding spectrum and its spectroscopic data obtained from NIST.
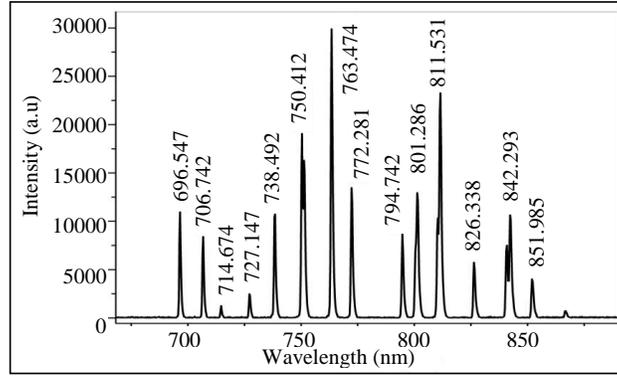

Figure 5: Argon glow discharge spectral lines

Table 1: Identified Argon peaks and its corresponding spectroscopic data

Wavelength λ / nm	Transitions	Statistical Weight g_k	Transition Probability A / s^{-1}	Upper level energy E_k / cm^{-1}
675.327	$3s^23p^5(^2P^o_{3/2})4d^2[3/2]o{\rightarrow}s23p5(^2P^o_{3/2})4p^2[1/2]$	5	1.93 x 10^6	118 906.6110
687.207	$3s^23p^5(^2P^o_{3/2})4d^2[1/2]^o \rightarrow s^23p^5(^2P^o_{3/2})4p^2[1/2]$	3	2.78 x 10^6	118 651.3950
703.060	$3s^23p^5(^2P^o_{3/2})6s^2[3/2]^o \rightarrow s^23p^5(^2P^o_{3/2})4p^2[5/2]$	5	2.67 x 10^6	119 683.0821
811.531	$3s^23p^5(^2P^o_{3/2})4p^2[5/2] \rightarrow s^23p^5(^2P^o_{3/2})4s^2[3/2]^o$	7	3.31 x 10^7	105 462.7596
912.208	$3s^23p^5(^2P^o_{3/2})4p^2[1/2] \rightarrow s^23p^5(^2P^o_{3/2})4s^2[3/2]^o$	3	1.89 x 10^7	104 102.0990
922.495	$3s^23p^5(^2P^o_{3/2})4p^2[3/2] \rightarrow s^23p^5(^2P^o_{1/2})4s^2[1/2]^o$	5	5.03 x 10^6	106 237.5518

Accuracy of this method can be improved by selecting lines which has large difference in upper energy level as the equation is solely temperature dependent. For each peak, the corresponding spectroscopic constants such as transition probability, upper energy level, transitions, and statistical weight are acquired from NIST standard databases [29].

From Table 1, the lines 912.208 nm and 703.060 nm are selected as these lines have the largest difference in their upper energy level. Using equation (7);

$$\frac{I_1}{I_2} = \frac{g_1}{g_2} \frac{A_1}{A_2} \frac{\lambda_2}{\lambda_1} e^{\left[-\left(\frac{E_1-E_2}{kT}\right)\right]}$$

$$\frac{149}{5883} = \frac{5}{3} \frac{(2.67\times10^{6)}}{(1.89\times10^7)} \frac{(912.208\times10^{-9})}{(703.060\times10^{-9})} e^{\left[-\left(\frac{14.840-12.908}{kT}\right)\right]}$$

$$T = 0.776 eV \text{ or } 9004K$$

As mentioned in section 3.1, the ratio method can be used to investigate the optically thin condition of the spectral lines selected. From equation (7), by selecting two lines of the same species which have the same upper energy level will eliminate the exponential term allowing the determination of theoretical intensity ratio of the two lines using just the spectroscopic constants. Deviation of experimental ratio from theoretical one suggests optically thick condition hence by plotting the intensity ratio against time one can find the suitable time window when LTE condition holds for the two lines selected [21].

This method is applied in ref [22] and [25] to determine the electron temperature from laser induced plasma of aluminium and zinc. In [22], two lines of Zn(I) were used to calculate the electron temperature under LTE condition with an uncertainty of $\pm10\%$ contributed by uncertainties in transition probabilities and measurement of intensity. Similarly in [25], LTE condition were assessed via McWhirter's criterion and few Al(II) lines were selected and the upper energy level has largest difference of 3.65 eV which imply highest electron temperature measured to be about 6.3 eV. However in [30], ratio method is used to determine the excitation temperature of hydrogen utilizing H□ □and H□ lines from DC discharge of a system of molecules which consist of nitrogen-acetylene-argon and nitrogen-acetylene-helium. In this case, LTE condition does not hold for low pressure discharge plasma [7, 30].

4.2   Boltzmann Plot

From equation 6, minor rearrangement yields;

$$\frac{\lambda_{ji}I_{ji}}{hcA_{ji}g_j} = \frac{n}{U(T)} e^{-\frac{E_j}{kT}} \tag{8}$$

Taking natural logarithm on both side of equation (8) results in [1, 13, 21, 24, 26, 27, 30-32];

$$\ln\left(\frac{\lambda_{ji}I_{ji}}{hcA_{ji}g_j}\right) = -\frac{1}{kT}(E_j) + \ln\left(\frac{N}{U(T)}\right) \tag{9}$$

Equation 9 gives a linear relationship when $\ln\left(\dfrac{\lambda_{ji}I_{ji}}{hcA_{ji}g_j}\right)$ versus E_j is plotted, and the electron temperature T can be determine from the slope of the plot. Similarly, Boltzmann plot requires peaks that originated from the same atomic species and the same ionization stage. However, an advantage that Boltzmann plot has over the ratio method is that lines which are optically thick can be easily identifiable from the large deviation of the data points in the straight line fitting [3-5].

In reference [24], 17 neutral argon emission lines observed from LIP are used to construct Boltzmann plot to yield the electron temperature of 5676 ± 346 K. This method is applied in the determination of excitation temperature for non-LTE plasma such as ICP [13] and DC discharge plasma [30].

Table 2: Data for Boltzmann plot using the peak information in Table 1

Wavelength / nm	Intensity / a.u.	Energy level/cm^{-1}	Energy level / eV	$\ln\left(\dfrac{\lambda_{ji}I_{ji}}{hcA_{ji}g_j}\right)$
912.208	5 883	104 102.0990	12.908	33.797
811.531	23 271	105 462.7596	13.077	33.648
922.495	1625	106 237.5518	13.173	33.335
687.207	130	118 651.3950	14.713	31.619
675.327	118	118 906.6110	14.744	31.358
703.06	149	119 683.0821	14.840	31.307

From Table 1, necessary data for Boltzmann plot are tabulated in Table 2. Both the ratio method and Boltzmann plot yields the value of argon's excitation temperature at a similar order of magnitude that is 0.776 eV and 0.788 eV respectively. The uncertainty of the excitation temperature determined from these methods is estimated to be about 10% due to uncertainties in measured intensities and transition probabilities [22]. Boltzmann plot constructed from data in Table 2 are shown in Figure 6 and its corresponding linear fitting equation.
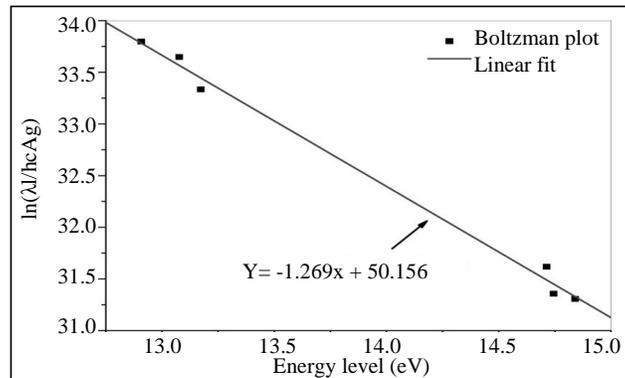

Figure 6: Boltzmann plot of Argon glow discharge using six Ar(I) lines

4.3   Saha-Boltzmann Equation

The Saha-Boltzmann equation considers the upper energy level to be the ionization stage, and hence the temperature calculated using this method is known as ionization temperature. Again, LTE condition dictates that the ionization temperature to be equal to the electron temperature. Unlike Boltzmann plot or ratio method which requires two spectral lines from the same species, Saha-Boltzmann equation utilizes spectral lines of the same element and successive ionization stages. From reference [21], the Saha-Boltzmann equation is given as;

$$n_e = \frac{I_z}{I_{z+1}^*} 6.04 \times 10^{21} (T)^{3/2} e^{\frac{(E_{j,z} - E_{j,z+1} - \chi_z)}{kT}} \ cm^{-3} \tag{10}$$

Where $I_z^* = I_z \lambda_{ji,z} / g_{j,z} A_{ji,z}$, χ_z is the ionization energy of the species in ionization stage z in eV, T_z is the line intensity for transition from upper level-j to lower level-i, $\lambda_{ji,z}$ is the corresponding wavelength of transition from level-j to level-i, $g_{j,z}$ is the statistical weight of transition from level-j, $A_{ji,z}$ is the transition probability from level-j to level-i and T is the electron temperature.

The subscript z denotes the ionization stage of the species for the referred. However, the use of Saha-Boltzmann to determine the electron temperature requires the knowledge of electron density. For that matter, this equation can work in both directions such that one can also determine the electron density with the knowledge of electron temperature. This equation could also be further extended such that it is similar to Boltzmann plot where the line slope corresponds to electron temperature which is discussed in detailed in reference [1].

4.4   Doppler Broadening

When the spectral line profile shows a Gaussian profile, this suggests that pressure and Doppler broadening dominate the plasma. Equation (11) is derived in reference [3, 5] for Doppler broadening which is given as;

$$\Delta \lambda_{1/2} = 2\lambda \sqrt{\frac{2kT_p \ln 2}{mc^2}} \tag{11}$$

where k is Boltzmann constant, m is the atomic mass, c is the speed of light, T_p is the plasma temperature, $\Delta \lambda_{1/2}$ is the FWHM of Doppler broadened spectral line, and λ is the central wavelength value of the peak.

N.M Shaikh *et al* [25] demonstrated this relationship in assessing the dominance of pressure broadening in laser induced plasma and found that it only contributes a small fraction of broadening mechanism as the plasma is heavily dominated by Stark broadening. Where as in [12, 13] this method is used to determine the inductively

coupled plasma temperature such that the FWHM value is obtained via curve fitting of Doppler spectral line.

5.   MEASUREMENT OF ELECTRON DENSITY

In this section, different techniques to obtain the electron density of plasma namely the Stark broadening relationship, and Saha-Boltzmann equation are discussed. Note that there are other available methods that have been successfully applied to calculate electron density such as line-continuum spectra [11] or Thompson scattering as demonstrated in [23] to measure the transient electron density for laser induced plasma. Another alternatives based on numerical modeling of plasma using collisional radiative model has also been utilized in determining electron density of laser induced plasma [28] and inductively driven plasma [12].

5.1   Stark Broadening

As discussed in section 3.3, Stark broadening caused by electric field of ions and electrons will lead to spectral broadening with FWHM given by equation 12 [2, 22, 25, 31];

$$\Delta\lambda_{\frac{1}{2}} = 2\omega\left(\frac{N_e}{10^{16}}\right) + 3.5\hat{A}\left(\frac{N_e}{10^{16}}\right)^{\frac{1}{4}}\left(1 - 1.2N_D^{-\frac{1}{3}}\right)\omega\left(\frac{N_e}{10^{16}}\right) \tag{12}$$

Where $\Delta\lambda_{\frac{1}{2}}$ is the FWHM of Stark broadened spectral peak, N_e is the electron density, ω is the electron impact parameter and N_D is the Debye shielding parameter.

The first and second term of equation (12) refers to broadening contributed by electron and ion respectively, and N_D also known as the number of particles in the Debye sphere which is dependent on electron density and electron temperature as follows [2, 25, 31];

$$N_D = 1.72 \times 10^9 \left(\frac{T^{\frac{3}{2}}}{N_e^{\frac{1}{2}}}\right)$$

However, equation 5.1 usually can be simplified by neglecting the second term because the broadening contribution is insignificant compared to that of electron which is used by many researchers as given by equation (13) [1, 2, 22-27, 31, 33];

$$\Delta\lambda_{\frac{1}{2}} = 2\omega\left(\frac{N_e}{10^{16}cm^-}\right) \tag{13}$$

The limitation of this technique is that one requires the knowledge of the value for the electron impact constant and in this case reference [34] gives a good compilation on the data for Stark width and shifts for most elements and its corresponding value of electron impact parameter. As shown by Giacomo et al in [28], the spectral profile can be

61

determined via normalized Voigt profile parameter R, which is equal to ratio of Lorentzian and Gaussian widths of the spectral line obtained via curve fitting of Voigt function such that the profile typology is Lorentzian dominated if R is greater than 0.4 and Gaussian dominated if R is less than 0.4.

In most researches, this method is applied to determine the electron density from laser induced plasma, however it is also applied in focused plasma in reference [33] using Ar(I) and Ar(II) emission lines and found the electron density to be $5.0 \times 10^{16} cm^{-3}$ and $4.7 \times 10^{16} cm^{-3}$ respectively.

5.2   Saha-Boltzmann Equation

In section 4.3, equation 4.5 was used to determine the electron temperature or excitation temperature with the prior knowledge of electron density. Thus, if the value of temperature is known, one can then find the electron density directly from the equation provided emission lines from the same species of successive ionization stage were present [1].

6.   CALIBRATION CURVE

For elemental recognition, it is generally agreed that at least three lines of the sample must match that of the known element to conclude that the sample contains that particular element or via signature wavelength for instance hydrogen is presence of H_α line that ensure the existence of hydrogen in the plasma. In order to measure the amount of an element that is present in the plasma source, calibration curve is commonly used. However a calibration-free method has been proposed as an alternative approach for quantification purpose in laser induced plasma and discussed in great detail by Tognoni and Ciucci A. *et al*. [32, 35].

Calibration curve is constructed using high purity samples of known concentration which is commonly used in LIBS study [8, 9]. The intensity of plasma emitted by each of these samples is plotted as a function of concentration. Hence, by measuring the experimental intensity of a spectral line of known element, one can deduce the concentration of the element from the calibration curve. As shown in [8] where LIBS technique was applied to for quantification of heavy metal elements in paint manufacturing plant wastewater, the calibration curve was constructed using four samples in powder form of 99.99% purity with concentrations that varies from 10, 1, 0.1 and 0.01 by weight percent of the elements. The results obtained were found to be in good agreement with the results measured via standard method like inductively coupled plasma spectrometer.

7. CONCLUSION AND FUTURE PROSPECT

This paper has reviewed the basic analytical techniques in plasma diagnostics via optical emission spectroscopy for any researchers who wish to venture into this field. Conditions for LTE plasma can be assessed using McWhirter's criterion or comparison of electron temperature determined using ratio method and Saha-Boltzmann equation. Optically thin condition of a spectral line can be gauged using Boltzmann plot and it can be determined qualitatively based on theoretical calculation via ratio method. For determination of plasma temperature, each method have its own advantages in terms of spectroscopic data available, or condition of spectral line profile such as Doppler mechanism dominated plasma allows for temperature measurement via FWHM of Doppler broadened peak. Saha-Boltzmann equation shows its versatility as a tool to determine either temperature or electron density with the knowledge of either one of the parameter.

The versatility of OES to determine plasma parameters is evident as it can be applied for any material research that involve the formation of plasma such as Laser Induced Breakdown Spectroscopy as mentioned earlier in this review. Current research thrust of our group aim to employ OES as a method to monitor the plasma parameter in a thin film deposition process and study its correlation with film properties as an alternative to material characterization procedures.

REFERENCES

[1]   Aragon C. and Aguilera J. A. (2008). Characterization of laser induced plasma by optical emission spectroscopy: a review of experiments and methods. *Spectrochimica Acta Part B.* Vol. 63, pp 893-916.

[2]   Fantoni R. *et. al* (2006). Laser induced breakdown spectroscopy (LIBS): The process, applications to artwork and environment. *Advances in Spectroscopy for Lasers and Sensing.* pp 229-254. Springer.

[3]   Griem H. R. (1997). *Principles of Plasma Spectroscopy.* Cambridge, United Kingdom. Cambridge University Press.

[4]   Hutchinson I. H. (2005). *Principles of plasma diagnostics*. (Second edition). United States of America: Cambridge University Press.

[5]   Kunze H. J. (2009). *Introduction to Plasma Spectroscopy*. London, New York. Springer Series on Atomic, Optical and Plasma Physics.

[6]   Marr G. V. (1968). *Plasma spectroscopy.* Great Britain: Elsevier Publishing Company Ltd.

[7]   Bogaerts A. *et al.* (2002). Gas discharge plasmas and their applications. *Spectrochimica Acta Part B,* Vol. 57, pp 609-658.

[8]   Gondal M. A. and Hussain T. (2007). Determination of poisonous metals in wastewater collected from paint manufacturing plant using laser induced breakdown spectroscopy. *Talanta*. Vol. 71, pp 73-80.

[9]   Trevizan L. C. *et al.* (2009). Evaluation of laser induced breakdown spectroscopy for the determination of micronutrients in plant materials. *Spectrochimica Acta Part B*. Vol. 64, pp 369-377.

[10]   Unnikrishnan V. K. *et al.* (2010). Optimized LIBS setup with echelle spectrograph-ICCD system for multi elemental analysis. *Jinst IOP Science.*

[11]   Bastiaans G. J. and Mangold R. A. (1985). The calculation of electron density and temperature in Ar spectroscopic plasmas from continuum and line spectra. *Spectrochimica Acta,* Vol. 40B, No. 7, pp 885-892.

[12]   Iordanova S. and Koleva I. (2007). Optical emission spectroscopy diagnostics of inductively-driven plasmas in argon gas at low pressures. *Spectrochimica Acta Part B,* Vol. 62, pp 344-356

[13]   Okada A. and Kijima K. (2002). Analysis of optical emission spectra from ICP of $Ar-SiH_4-CH_4$ system. *Vacuum,* Vol. 65, pp 319-326.

[14]   E.H. van Veen and M. T. C. de Loos-Vollebregt (1998). Application of mathematical procedures to background correction and multivariate analysis in inductively coupled plasma-optical emission spectrometry. *Spectrochimica Acta Part B,* Vol. 53, pp 639-669.

[15]   Weiss Z. (2006). Emission yields and the standard model in glow discharge optical emission spectroscopy: Links to the underlying physics and analytical interpretation of the experimental data. *Spectrochimica Acta Part B,* Vol. 61, pp121-133.

[16]   Bogaerts A. *et al.* (2001). Comparison of modeling calculations with experimental results for direct current glow discharge optical emission spectrometry. *Spectrochimica Acta Part B,* Vol. 56, pp 551-564.

[17]   Bogaerts A. and Gijbels R. (2003). Numerical modeling of gas discharge plasmas for various applications. *Vacuum,* Vol. 69, pp 37-52.

[18]   Adams M. J. (2004). *Chemometrics in Analytical Spectroscopy*. The Royal Society of Chemistry, Cambridge.

[19]   Gurnett D. A. and Bhattacharjee A. (2005). *Introduction to plasma physics: with space and laboratory applications.* United Kingdom: Cambridge University Press.

[20]   Bellan P. M. (2006). *Fundamental of plasma physics.* United States of America: Cambridge University Press.

[21]   Unnikrishnan V. K. et al (2010). Measurement of plasma temperature and electron density in laser-induced copper plasma by time-resolved spectroscopy and neutral atom and ion emissions. *Praman Journal of Physics*. Vol. 75 No. 6, pp 983-993.

[22]   Abdellatif G. and Imam H. (2002). A study of the laser plasma parameter at different laser wavelengths. *Spectrochimica Acta Part B*. Vol. 57, pp 1155-1165.

[23]   Diwakar P. K. and Hahn D. W. (2008). Study of early laser-induced plasma dynamics: transient electron density gradient via Thomson scattering and Stark broadening, and the implications on laser-induced breakdown spectroscopy measurements. *Spectrochimica Acta Part B.* Vol. 63, pp 1038-1046.

[24]   L. Cadwell and L. Huwel (2004). Time-resolved emission spectroscopy in laser-generated argon plasmas-determination of Stark broadening parameters. *Journal of Quantitative Spectroscopy & Radiative Transfer*. Vol. 83, pp 579-598.

[25]   Shaikh N. M. et al (2006). Measurement of electron density and temperature of a laser-induced zinc plasma. *Institute of Physics Publishing, Journal of Physics D: Applied Physics*. Vol. 39, pp 1384-1391.

[26]   Tawfik W. and Askar A. (2007). Study of the matrix effect on the plasma characterization of heavy elements in soil sediments using LIBS with a portable echelle spectrometer. *Progress in Physics*, Vol. 1, pp 46-52.

[27]   Tawfik W. (2007). Study of the matrix effect on the plasma characterization of six elements in aluminum alloys using LIBS with a portable echeele spectrometer. *Progress in Physics,* Vol. 2, pp 42-48.

[28]   [28]   Giacomo A. D. *et. al* (2001). Optical emission spectroscopy and modeling of plasma produced by laser ablation of titanium oxides. *Spectrochimica Acta Part B.* Vol. 56, pp 753-776.

[29]   Ralchenko, Yu., Kramida, A.E., Reader, J., and NIST ASD Team (2011). *NIST Atomic Spectra Database* (ver. 4.1.0), [Online].   http://physics.nist.gov/asd3. National Institute of Standards and Technology, Gaithersburg, MD.

[30] Jamroz P. and Zyrnicki W. (2010). Optical emission spectroscopy study for nitrogen-acetylene-argon and nitrogen-acetylene-helium 100kHz and dc discharges. *Vacuum,* Vol. 84, pp 940-946.

[31] Diao C. Y. *et al.* (2011). Influence of distances between the lens and the target on the characteristic of laser induced lead plasma. *The European Physical Journal D*. Vol. 63, pp 123-128.

[32] Tognoni E. *et al.* (2007). A numerical study of expected accuracy and precision in calibration-free Laser-induced Breakdown Spectroscopy in the assumption of ideal analytical plasma. *Spectrochimica Acta Part B,* Vol. 62, pp 1287-1302.

[33] Young J. H. *et al.* (2010). Measurement of electron temperature and density using Stark broadening of the coaxial focused plasma for extreme ultraviolet lithography. *IEEE Transactions on Plasma Science*. Vol. 38, No 5, pp. 1111-1117.

[34] Konjevic N. *et. al* (2002). Experimental stark widths and shifts for spectral lines of neutral and ionized atoms. *Journal of Physical Chemistry Ref. Data.* Vol. 31 no.3.

[35] Ciucci A. *et al.* (1999). New procedure for quantitative elemental analysis by laser induced plasma spectroscopy. *Applied Spectroscopy*, Vol. 53, no. 8, pp 960-964.